NeuroImage 199 (2019) 427–439

Contents lists available at ScienceDirect

NeuroImage

journal homepage: www.elsevier.com/locate/neuroimage

High-fidelity mapping of repetition-related changes in the parietal memory network

Adrian W. Gilmore [a,*], Steven M. Nelson [h,i,j], Timothy O. Laumann [b,c], Evan M. Gordon [h,i], Jeffrey J. Berg [a], Deanna J. Greene [c,d], Caterina Gratton [b], Annie L. Nguyen [b], Mario Ortega [b], Catherine R. Hoyt [b,g], Rebecca S. Coalson [b,d], Bradley L. Schlaggar [b,k,l,m], Steven E. Petersen [a,b,d,e], Nico U.F. Dosenbach [b,d,f,g], Kathleen B. McDermott [a,d]

[a] Department of Psychological and Brain Sciences, Washington University in St. Louis, St. Louis, MO, 63130, USA
[b] Department of Neurology, Washington University School of Medicine, St. Louis, MO, 63110, USA
[c] Department of Psychiatry, Washington University School of Medicine, St. Louis, MO, 63110, USA
[d] Department of Radiology, Washington University School of Medicine, St. Louis, MO, 63110, USA
[e] Department of Neuroscience, Washington University School of Medicine, St. Louis, MO, 63110, USA
[f] Department of Pediatrics, Washington University School of Medicine, St. Louis, MO, 63110, USA
[g] Program in Occupational Therapy, Washington University School of Medicine, St. Louis, MO, 63110, USA
[h] VISN 17 Center of Excellence for Research on Returning War Veterans, Waco, TX, 76711, USA
[i] Center for Vital Longevity, University of Texas at Dallas, Dallas, TX, 75235, USA
[j] Department of Psychology and Neuroscience, Baylor University, Waco, TX, 76798, USA
[k] Kennedy Krieger Institute, Baltimore, MD, 21205, USA
[l] Department of Neurology, Johns Hopkins University School of Medicine, Baltimore, MD, USA
[m] Department of Pediatrics, Johns Hopkins University School of Medicine, Baltimore, MD, USA

ARTICLE INFO

Keywords:
Familiarity
fMRI
Highly-sampled human subjects
Memory
Parietal cortex
Retrieval

ABSTRACT

fMRI studies of human memory have identified a "parietal memory network" (PMN) that displays distinct responses to novel and familiar stimuli, typically deactivating during initial encoding but robustly activating during retrieval. The small size of PMN regions, combined with their proximity to the neighboring default mode network, makes a targeted assessment of their responses in highly sampled subjects important for understanding information processing within the network. Here, we describe an experiment in which participants made semantic decisions about repeatedly-presented stimuli, assessing PMN BOLD responses as items transitioned from experimentally novel to repeated. Data are from the highly-sampled subjects in the Midnight Scan Club dataset, enabling a characterization of BOLD responses at both the group and single-subject level. Across all analyses, PMN regions deactivated in response to novel stimuli and displayed changes in BOLD activity across presentations, but did not significantly activate to repeated items. Results support only a portion of initially hypothesized effects, in particular suggesting that novelty-related deactivations may be less susceptible to attentional/task manipulations than are repetition-related activations within the network. This in turn suggests that novelty and familiarity may be processed as separable entities within the PMN.

1. Introduction

For over two decades, PET and fMRI experiments have linked activity within parietal cortex to the retrieval of information from episodic memory (e.g., Tulving et al., 1994; McDermott et al., 1999; Wiggs et al., 1999; for reviews, see Wagner et al., 2005; Ciaramelli et al., 2008; Vilberg and Rugg, 2008; Nelson et al., 2013b; Rugg and King, 2017; Sestieri et al., 2017). However, articulating specific parietal contributions to memory retrieval has proven to be difficult. In part, this difficulty is due to a lack of convergent evidence from the neuropsychology literature: patients with parietal lobe lesions do not display pronounced memory deficits (Berryhill et al., 2007; Davidson et al., 2008; Olson and Berryhill, 2009; Berryhill, 2012; for a recent exception, see Ben-Zvi et al., 2015). Instead, the minor memory deficits that are observed typically relate to a

* Corresponding author. 10 Center Drive, MSC1366, Building 10, Room 4C104, Bethesda, MD, 20892, USA.
E-mail address: adrian.gilmore@nih.gov (A.W. Gilmore).

https://doi.org/10.1016/j.neuroimage.2019.06.011
Received 21 December 2018; Received in revised form 3 June 2019; Accepted 4 June 2019
Available online 5 June 2019
1053-8119/Published by Elsevier Inc.

patient's confidence in—rather than the contents of—retrieved information. In addition, the spatial extent of retrieval-related activation within the parietal lobe is often vast, covering many of the small, interdigitated parcels that comprise both lateral and medial parietal cortex (Nelson et al., 2010; Seghier, 2013; Yang et al., 2014; Bzdok et al., 2015; Braga and Buckner, 2017). Thus, associating retrieval-related activity with the underlying functional architecture of parietal cortex has been challenging (Cabeza et al., 2012; Nelson et al. 2012, 2013b; Sestieri et al., 2017).

One approach to understanding parietal contributions to retrieval is to focus on smaller, more precisely specified regions of cortex. This approach can particularly benefit from a recent trend toward studies employing small numbers of participants with large amounts of data per person (Laumann et al., 2015; Braga and Buckner, 2017; Gordon et al., 2017b; Gratton et al., 2018; Marek et al., 2018), particularly when these are combined with a clearly hypothesized prediction regarding activity within a single region or set of regions that is fairly small or circumscribed.

One such collection of regions consists of the parietal memory network (PMN), which is a sparse cortical network that has recently been associated with the processing of stimulus novelty or familiarity (Gilmore et al. 2015, 2019; McDermott et al., 2017). Regions within this network—which fall within the posterior inferior parietal lobule/dorsal angular gyrus (pIPL/dAG), the precuneus (PCU), and the mid-cingulate cortex (MCC)—are among those that most reliably exhibit retrieval success effects (e.g., Wagner et al., 2005; Spaniol et al., 2009; Kim, 2013). Furthermore, these regions tend to display an "encoding/retrieval flip" (Vannini et al., 2011; Huijbers et al., 2013) such that they typically deactivate in response to novel stimuli but activate above resting-baseline levels for previously-studied experimental stimuli (Gilmore et al., 2015; McDermott et al., 2017). Both meta-analytic studies of fMRI task data (e.g., Kim, 2013) and studies employing functional connectivity data (e.g., Yang et al., 2014) have indicated that PMN regions are adjacent to, but distinct from, larger default network regions such as those within the posterior cingulate cortex or angular gyrus (see also Power et al., 2014b; Gilmore et al., 2015). However, the larger areal extents of default regions when compared to PMN regions makes visual identification potentially challenging in task-only contexts and suggests that alternative localization approaches might be useful.

An important property of the PMN appears to be the largely "bottom-up" nature of its activity: repetition enhancement effects appear to be present if one observed experimental stimuli multiple times in the context of a single experiment, even if these repetitions are not accompanied by explicit retrieval instructions (Nelson et al., 2013a; Brodt et al., 2016; Gilmore et al., 2019; see also Elman and Shimamura, 2011). Combined with the typical encoding/retrieval flip associated with PMN regions, it raises the possibility that one might effectively localize the PMN using a task in which no explicit retrieval component is necessary at the level of the individual, in a manner that separates it from surrounding cortex.

This possibility was explored in the current experiment. Subjects viewed stimuli repeatedly, making a basic semantic category decision each time a stimulus was encountered. Three predicted patterns—deactivation in response to novel stimuli, repetition-related changes in activity, and above-baseline activations in response to familiar items—were directly examined. Differences in activity were compared between initial and final presentations for each stimulus, so that activity for novel and familiar items could be directly contrasted. Data for this experiment are publicly available as a part of the "Midnight Scan Club" dataset (Gordon et al., 2017b), accessible in raw and preprocessed form at the Openfmri repository (https://openfmri.org/dataset/ds000224/; Poldrack et al., 2013). This dataset therefore contains large amounts of task data for each of the 10 included subjects (30 relevant scan runs per person, totaling approximately 2.5 h of fMRI data). Importantly, the large amount of data per subject allowed for PMN regions to be identified at the level of the individual as well as the entire group. Similarity in responses observed at the group and single-subject levels would provide a bridge between results that might be obtained in a "typical" group design and those obtained using a small N, high-data approach; this approach could further help allay concerns that previously-observed responses might be due to blurring across multiple, adjacent regions (Nelson et al., 2010). In addition to the large amount of task data, 5 h of resting-state data were collected per subject so that the PMN could be independently identified via resting-state functional connectivity mapping. We were therefore able to define regions in multiple ways and rely on converging evidence to address the nature of repetition-related effects within the PMN in the experimental task.

2. Methods

2.1. Subjects

All subjects (N = 10) contributing to this dataset were described by Gordon et al. (2017b). Two of these subjects were members of the research team, and all were right-handed. Demographic information for all subjects is included in Table 1. Informed consent was obtained from all subjects in accordance with standard Washington University human research practices. Monetary compensation was provided to the eight subjects who were not members of the research team. All sessions for all subjects were collected at the same time of day (midnight). Additional details related to data collection, including other task conditions not discussed in this report, are described in Gordon et al. (2017b).

2.2. Materials

2.2.1. Faces

Face stimuli consisted of 240 photographic images of male and female faces (120 of each), taken from publicly available electronic databases. These included Stirling's 2D face set from the Psychological Image Collection (http://pics.stir.ac.uk); the CNBC Tarrlab "Face Place" repository (http://wiki.cnbc.cmu.edu/TarrLab; Righi et al., 2012); the Park Aging Mind Laboratory Face Database (http://agingmind.utdallas.edu/facedb); and Libor Spacek's Facial Images Database (http://cmp.felk.cvut.cz/~spacelib/faces; Hond and Spacek, 1997). Faces were organized into 10 lists of 24 faces (half male, half female). All faces within a single list were drawn from the same database to maximize within-list consistency of image quality. Images were resized to a 4:3 aspect ratio and were presented as a 600 x 450 pixel image in the center of the screen (overall screen resolution: 1024 x 768 pixels).

2.2.2. Scenes

Scene stimuli consisted of 240 photographic images of indoor and outdoor scenes (120 of each), taken from a larger stimulus set originally reported in Chen et al. (2017). Stimuli were organized into 10 lists of 24 scenes, half indoor and half outdoor. All photographs were originally 800

Table 1
Subject demographic information.

Subject	Age	Gender	Years of Education	KBIT Verbal IQ score	KBIT Nonverbal IQ score
S01	34	M	22	129	125
S02	34	M	28	129	130
S03	29	F	18	117	112
S04	28	F	22	127	130
S05	27	M	20	102	132
S06	24	F	17	119	125
S07	31	F	20	127	132
S08	27	F	21	129	115
S09	26	M	19	135	115
S10	31	M	19	135	132
Average	29.1	n/a	20.6	124.9	124.8

x 600 pixels or larger in size to ensure sufficiently high image quality, and no humans were visible in any of the pictures. Scenes were cropped to a 4:3 aspect ratio and presented as a 600 x 450 pixel image in the center of the screen. An additional list of 24 images (half indoor, half outdoor) were used in a make-up session for S02 to replace a task run corrupted by a software malfunction.

2.2.3. Words

Word stimuli consisted of 240 nouns taken from the English Lexicon Project database (http://elexicon.wustl.edu; Balota et al., 2007). Words were 5–8 characters in length, 1–4 syllables in length, and had an average HAL frequency rating (Lund and Burgess, 1996) of 5781.9 (range: 20–34727). 120 words were classified as concrete, and 120 as abstract, based on their MRC Psycholinguistic database concreteness ratings (http://websites.psychology.uwa.edu.au/school/MRCDatabase/uwa_mrc.htm; Wilson, 1988). Words with concreteness ratings <350 ($M = 292$; range: 204–349) were considered abstract, and those with ratings >525 ($M = 606$; range: 530–662) were considered concrete. Words within each list were balanced for character length, number of syllables, HAL frequency, and concreteness rating.

2.3. Experimental task

The task data reported here were collected as part of a larger protocol collected across 12 distinct scanning sessions as described in Gordon et al. (2017b). These data were acquired immediately after a 30-min rest scan but before any other tasks were completed. Subjects made binary semantic decisions about scenes, faces, and words, each of which were presented multiple times, as quickly as possible without sacrificing accuracy. Each scan run contained only a single stimulus type. The order in which each stimulus type appeared was rotated across days to avoid simple order effects. As there were three runs per session, a total of 30 task runs were collected for each subject. An exception to this was S10, for whom only 27 task scans were included for analysis due to a technical error.

In each task run, subjects viewed 24 stimuli (unique to that run), three times each. All stimuli were presented a single time before any were repeated, and all stimuli were shown twice before any were presented for a third time. This basic sequence repeated for all 3 task scans per session (see Fig. 1). Stimulus order was shuffled between presentations within each run to produce a different presentation order and ensure an approximately equal delay between occurrences across all items. Each stimulus was presented for 1700 ms against a black background, followed by a jittered inter-stimulus interval (ISI) ranging from 500 to 4900 ms. During the ISI, a white fixation cross (48-point Arial type) was presented in the center of the screen.

For faces, subjects were instructed to indicate, via button press, if the face was male or female. For scenes, they were instructed to indicate whether they were viewing an indoor or outdoor scene. For words, they indicated if they thought the word was abstract or concrete. In each case, subjects were directed to perform the task as directed regardless of the number of times a given item may have been seen in the experiment (for verbatim instructions given for each task, see Supplementary Materials). Subjects had 2200 ms from the onset of each stimulus to make their responses.

2.4. MRI data acquisition

Data were acquired using a Siemens MAGNETOM Tim Trio 3.0 T scanner using a 12-channel Matrix head coil (Erlangen, Germany). Subjects were situated in the scanner with foam pillows to help maintain subject comfort and stabilize head position. Four T1-weighted sagittal Magnetization-Prepared Rapid Gradient Echo (MP-RAGE) structural images were obtained for each subject (TE = 3.74 ms, TR(partition) = 2400 ms, TI = 1000 ms, flip angle = 8°, 224 slices with 0.8 x 0.8 × 0.8 mm voxels, FOV = 256 x 256) (Mugler and Brookerman, 1990). Four T2-weighted sagittal turbo spin echo structural images (TE = 479 ms, TR = 3200 ms, 224 slices with 0.8 x 0.8 × 0.8 mm voxels, FOV = 256 x 256) were also obtained for each subject. Gradient field maps were collected to estimate inhomogeneities in the magnetic field for each subject in each scanning session. An auto-align pulse sequence protocol provided in the Siemens software was used to align the acquisition slices of the functional scans parallel to the anterior commissure-posterior commissure (AC-PC) plane. Functional imaging was performed using a BOLD contrast sensitive gradient echo echo-planar sequence (TE = 27 ms, flip angle = 90°, in-plane resolution = 4 × 4 mm). Whole brain EPI volumes (MR frames) of 36 contiguous, 4-mm-thick axial slices were obtained every 2200 ms.

A headset with noise-canceling headphones was used to reduce in-scanner noise for all subjects. An Apple iMac computer (Apple, Cupertino, CA, USA) running PsyScope software (Cohen et al., 1993) was used to display stimuli. An LCD projector (Sharp model PG-C20XU) was used to project stimuli onto an MRI-compatible rear-projection screen (CinePlex) at the head of the bore, which the subjects viewed through a mirror attached to the head coil (maximum field of view = 21° of visual angle).

2.5. fMRI data preprocessing

Imaging data from each subject were pre-processed to reduce noise and to maximize across-session registration, using methods described in Laumann et al. (2016). Data from each session were corrected for within- and across-scan movement using a rigid-body rotation and translation

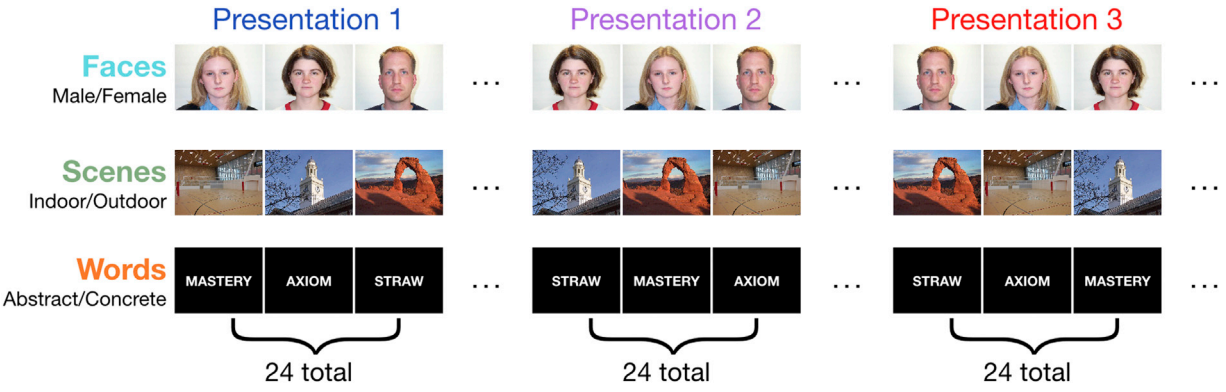

Fig. 1. Task design. In separate scan runs, participants made semantic decisions about faces, scenes, or words. Each stimulus was presented 3 times, and the same decision was made each time a given stimulus was observed. All stimuli were presented once before any were presented twice, and all were presented twice before any were presented for a third time.

algorithm (Snyder, 1996), and were intensity-normalized to a whole-brain mode 1000 to allow for comparisons across runs and subjects (Ojemann et al., 1997). Transformation of functional data to a target atlas space (711-2 B) was computed by registering the mean intensity image from each subject's first functional scan to atlas space via the average T1-and T2-weighted images ($n = 4$ for each image type). All other BOLD runs for each subject were linearly registered to this first session. Atlas transformation, distortion correction using a mean field map (Laumann et al., 2015), and resampling to a 3 mm isotropic atlas space were combined into a single interpolation step using the *applywarp* tool in FSL (Smith et al., 2004). Subsequent analyses were performed on the atlas-transformed data within and across subjects. No additional smoothing (beyond that implicit in the above transformations) was applied during initial preprocessing.

2.6. GLM-based fMRI data analysis

Time series data were analyzed using a general linear model (GLM; Friston et al., 1994; Miezin et al., 2000), in which the data for each time point in each voxel are treated as the sum of all effects present at that time point. The time course of activity for effects in each condition was modeled as a set of delta functions following the onset of each coded event (Ollinger et al. 2001a, 2001b). This approach assumes that all events associated with a specific condition evoke the same BOLD response but makes no assumptions of what the shape of that response might be. Regressors reflect distinct task conditions as well as effects of non-interest, as described below.

2.7. Group GLM creation and analysis parameters

Each task scan consisted of 121 frames. This was reduced to 117 after discarding the first 4 frames of each run to allow for T1 equilibration effects, and for each subject all 30 runs were concatenated into a single time series 3510 frames in length. Separate regressors coded for each presentation number (1–3) of each stimulus type (faces, scenes, and words), and each class of each stimulus type (e.g., both female and male faces). This resulted in 18 distinct event conditions per subject.[1] Each condition was modeled over 8 time points, capturing 17.6s of BOLD activity following trial onset. Additional regressors of non-interest for each run included a trend term to account for linear changes in signal, and a constant term modeling the baseline signal. For the group-level analysis described below (but no other analyses), a 6-mm Gaussian blur was applied to the voxelwise statistical maps for each subject to accommodate inter-subject anatomical differences.

2.8. ANOVA and t-test parameters

A multi-step approach was taken to identify voxels sensitive to stimulus repetition effects. First, a Presentation (1–3) x Time Point (1–8) ANOVA (collapsing across all stimulus types) was conducted to identify voxels whose time course of activity changed across stimulus presentations. In order to correct for multiple comparisons and achieve a whole-brain familywise error rate (FWE) of $p < .05$, only voxels with a z-score exceeding 3, and that were contiguous with at least 13 other such voxels, were considered to be significant (McAvoy et al., 2001).

Within each voxel identified by the Presentation x Time Point ANOVA, a *t*-test (paired-samples, two-tailed) was conducted to provide information about the directionality of the difference across presentations. This contrasted activity between Presentation 3 (for all stimulus types) and Presentation 1 (all stimulus types) across Time Points 3–5 (4.4–11.0 s following trial onset). We chose to collapse across stimulus type because our primary interest was in general effects of repetition, rather than those related to faces, scenes, or words *per se*. A subsequent threshold of $|z| > 1.96$ (corresponding to an uncorrected $p < .05$) was applied in this step, as the initial ANOVA maps had already been corrected to a FWE of $p < .05$, as described above. All voxels considered significant at this point therefore demonstrated a significant interaction of Presentation number and Time Point, and also exhibited significantly different activity between Presentation 3 and Presentation 1 during their peak response period.

2.9. ROI definition

An automated peak searching algorithm (peak_4dfp) searched the contrast maps for local maxima, around which spherical ROIs were drawn. Peaks under 10 mm apart were consolidated via coordinate averaging. ROIs were then obtained by centering an 8-mm diameter sphere about the identified coordinates. Putative PMN ROIs were identified by selecting the closest ROI to each canonical PMN region (left pIPL/dAG, left PCU, MCC) as well as homotopic (x-flipped) coordinates on the right hemisphere for pIPL/dAG and PCU. Time courses were extracted from each ROI by averaging activity across all included voxels. *A priori* coordinates were based on those used in McDermott et al. (2017), which themselves were based on a synthesis of several prior meta-analyses (specifically, McDermott et al., 2009; Nelson et al., 2010).

2.10. Single-subject GLM creation and analysis parameters

A secondary analysis was conducted at the single-subject level. Here, the three runs for each session were concatenated together, creating 10 time series of 351 MR volumes. In this analysis, sessions, rather than subjects, were treated as a random effect. Conditions were modeled as they were in the group level analyses. The same approach was taken to identify voxels sensitive to stimulus effects: an initial ANOVA ($z > 3$, $k \geq 3$) identified voxels which were later analyzed via *t*-test (paired samples, two-tailed, $|z| > 1.96$) to identify how activity differed as a function of stimulus presentations. ROI definition for each PMN region of each subject occurred as described previously, with the additional constraint that at least one peak had to be located within 15 mm of an *a priori* coordinate or the specific ROI would be excluded for a given subject. We note here that we did not perform any additional smoothing for this analysis, to maximize anatomical specificity within each subject (albeit at the cost of additional thermal noise within each voxel).

2.11. Analysis and visualization software

Image processing was performed using Washington University's in-house fMRI processing software (FIDL; http://www.nil.wustl.edu/~fidl/) written in IDL (Research Systems, Inc.). For display purposes, statistical maps were sampled from volume to surface space and projected onto partially inflated surface representations of the human brain using Connectome Workbench software (Marcus et al., 2011). Coordinates were converted from 711 to 2 B space to MNI152 space for the purposes of reporting.

2.12. Resting-state functional connectivity preprocessing

Resting-state functional connectivity data have proven to be a strong complement to task fMRI data and are an effective means of independently identifying ROIs. In the case of the current experiment, the hypotheses being tested relate specifically to a single functional network that was initially identified using resting-state data to define network communities that preceded the network being ascribed a function (Doucet et al., 2011; Power et al., 2011; for additional discussion, see

[1] Additional GLMs were also created which only coded for Presentation Number (1–3) or Task Condition (Face, Scene, Word) and Presentation Number (1–3). These reduced complexity GLMs yielded extremely similar contrast maps to those reported here, both at the group and single-subject levels. The GLMs used here are also the same as those used to create the univariate maps uploaded to NeuroVault.

Power et al., 2014b; Gilmore et al., 2015). Thus, resting-state data collected as a part of the Midnight Scan Club protocol were of use in the current experiment as a means of verifying our localization of PMN regions. This verification step allowed us to examine repetition-related effects using a completely independent source of data and avoid concerns related to "double-dipping" from the task data (Kriegeskorte et al., 2009; Vul and Pashler, 2012).

Resting-state data initially underwent preprocessing as described for the task data, but several additional steps were taken to reduce artifacts within the BOLD time series for each subject. Steps included nuisance regression, frame censoring, interpolation, and spectral filtering (Power et al., 2014a). Nuisance regressors included the global gray matter, white matter, and ventricular signals and their first derivatives, and 24 parameters derived from estimated subject motion (translational and rotation x,y,z and their polynomial expansions; Friston et al., 1996). Masks for global gray matter, white matter, and ventricles were defined using FreeSurfer version 5.3 (https://surfer.nmr.mgh.harvard.edu/). Frames were censored if their framewise displacement (FD) exceeded 0.2 mm. If fewer than 5 contiguous frames were present in a portion of the time series, these sections were also censored. Interpolation over censored epochs (which was necessary for subsequent bandpass filtering) was computed by a least-squares spectral estimation (Power et al., 2014a; Laumann et al., 2016). Data were temporally filtered at $0.08 > f > 0.009$ Hz. Censored frames were not included in the final correlation calculations.

2.13. Sampling fMRI data to the cortical surface

After preprocessing, resting-state data were sampled to the cortical surface, following the methods of Laumann et al. (2016) (see also Glasser et al., 2013; Laumann et al., 2015). Surfaces were generated from the subject's mean MP-RAGE image using the FreeSurfer's *recon-all* processing pipeline. Steps included brain extraction, segmentation, generation of white matter and pial surfaces, inflation of the surfaces to a sphere, and registration of the spherical surface to the fsaverage surface (Dale et al., 1999; Fischl et al., 1999; Segonne et al., 2004). The two hemispheres were brought into common registration with one another via the "fs_LR" hybrid left-right fsaverage surface (Van Essen et al., 2012). Surfaces were initially resampled to a resolution of 164,000 vertices (164 k fs_LR) using CARET software (Van Essen et al., 2001) and were then downsampled to a resolution of 32,492 vertices (fs_LR 32 k). Transformation values from native surfaces to the fs_LR 32 k surface were composed into a single deformation map. All steps involved in this surface sampling were implemented with the Freesurfer_to_fs_LR Pipeline (http://brainvis.wustl.edu).

Following surface creation for each subject, their BOLD data were then sampled to their unique surfaces. The BOLD fMRI data were sampled to each subject's native mid-thickness surface using the ribbon-constrained sampling procedure from the Connectome Workbench software package (Marcus et al., 2011). This sampled data from voxels located within the mid-thickness surface ribbon (i.e., the space between the white and pial surfaces) and weighted each voxel by its location within the ribbon. Voxels were excluded if they had a coefficient of variation 0.5 standard deviations higher than the mean coefficient of neighboring voxels within a 5 mm Gaussian circle (Glasser et al., 2013). After being sampled to the native surface, time courses were deformed and resampled onto the 32 k fs_LR surface using the subject-specific deformation map described above. After sampling to a common surface space, all data were geodesically smoothed using a Gaussian kernel ($\sigma = 2.55$ mm).

Surface data from each subject were then combined with data from subcortical structures and the cerebellum into a single CIFTI file using Connectome Workbench software. The resulting file thus contained all cortical and subcortical gray matter tissue for each participant. Volumetric data were smoothed using a 2.55 mm spherical Gaussian kernel to ensure consistency with the surface data.

2.14. Network community assignment

Resting-state network communities were first defined within each subject using a template matching procedure previously described by Gordon et al. (2017a). This approach capitalizes on the known group-level network structure of the human brain and assigns each vertex to a specific network based on the similarity of its correlation pattern in a winner-take-all manner. Previous work has indicated that this procedure is sensitive to individual differences in the extent and location of network parcels—even if these fall outside the expected "canonical" locations—and has been shown to do so even with substantially less data than was available in the current dataset (Gordon et al., 2017a). The template used in this matching procedure was derived from group-averaged network communities estimated in 120 subjects (Power et al., 2011; Gordon et al., 2017a).

The BOLD time series for each of the ten 30-min resting-state scans were concatenated, and a cross-correlation matrix of edge connections was computed for all nodes (i.e., vertices). The time series from each vertex was then correlated against all other vertices, and the resulting matrix was Fisher z-transformed, thresholded at the top 0.5% of connectivity values, and binarized. The dice coefficient of overlap was calculated between the binarized map and a series of binarized templates from the 120-subject discovery sample, and the template with the highest overlap was used to assign system membership in a winner-take-all fashion. To exclude matches driven by purely local connectivity, all vertices within 25 mm geodesic distance from the selected vertex were excluded from the matching process. System areas which were less than 25 mm^2 were ignored, and adjacent systems were expanded in a vertexwise fashion until the empty patch was filled. Each individual's PMN was then resampled into 711-2 B volume space, and spherical ROIs (4 mm radius) were centered on each cluster's center of mass within each subject. Time courses were extracted, and responses were tested as described previously.

In a separate analysis, resting-state network communities were also defined within each subject using the Infomap algorithm (Rosvall and Bergstrom, 2008), following procedures used by Laumann et al. (2015). The BOLD time series data from each session were concatenated for each subject, and a cross-correlation matrix of edge connections was computed for all included nodes. Nodes included both surface vertices and subcortical voxels. Node connections within 10 mm of one another (geodesic distance for vertices, Euclidian distance for voxels) were removed to avoid spurious correlation values resulting from the applied spatial smoothing. System assignments were computed across 46 thresholds ranging from 0.05 to 5.0% edge densities (in steps of .01%). Network communities consisting of 400 or fewer nodes, and all subcortical or cerebellar voxels, were not further considered in this analysis. Network communities for each subject were labeled according to a "consensus" assignment (for details, see Laumann et al., 2015; Gordon et al., 2017b) by minimizing distance metrics across all communities. Each individual's PMN was then resampled into 711-2 B volume space, and spherical ROIs (4 mm radius) were centered on each cluster's center of mass within each subject. Time courses were extracted, and responses were tested as described previously.

3. Behavioral results

3.1. Subjects were accurate in their classifications

Subjects were effectively at ceiling in their classifications for all types of stimuli (Fig. 2, top). On average, they responded correctly on 97.3% (*SEM* = 0.19%) of trials. Focusing on individual stimuli, faces were correctly classified as male or female 98.5% of the time (*SEM* = 0.21%), scenes were correctly classified as indoor or outdoor 97.0% of the time (*SEM* = 0.17%), and words were correctly classified as abstract or concrete 96.5% of the time (*SEM* = 0.43%).

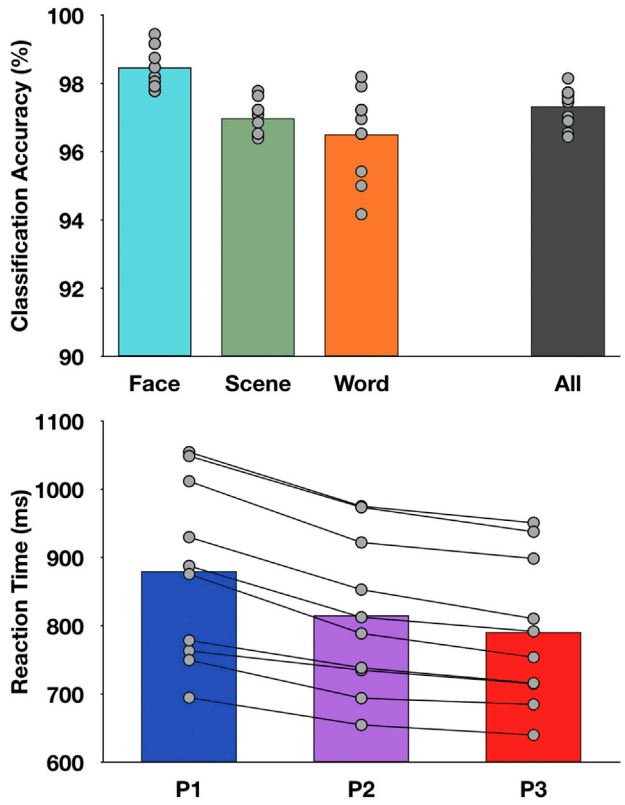

Fig. 2. Behavioral response data. Top: Subjects were accurate in their classification of all stimulus types. Bottom: Subjects demonstrated faster responses across stimulus presentations. Bars reflect group mean, and dots reflect values from each subject.

3.2. Response times improved across stimulus presentations

Subjects responded more rapidly as they repeatedly made the same type of judgment for each stimulus (Fig. 2, bottom; Fig. S1, top). This pattern was observed when advancing from Presentation 1 to Presentation 2 (879.8 vs. 815.1 ms), as well as from Presentation 2 to Presentation 3 (815.1 vs. 790.5 ms). Planned comparisons using two-tailed, paired-samples *t*-tests verified the significance of these results (least significant difference: $t(9) = 7.75$, $p < .001$; obtained for Presentation 2 vs. Presentation 3 comparison).

One might expect that generalized practice effects would manifest across the 10 experimental sessions, such that RTs could change from day to day as the experiment progressed. However, no evidence of such practice effects was observed (Supplementary Fig. S1, bottom). A 3 (Presentation number) x 10 (Session number) ANOVA indicated a main effect of Presentation, $F(2,10.1) = 89.80$, $p < .001$ (Greenhouse-Geisser corrected for nonsphericity), but no main effect of Session $F(9,81) = 1.17$, $p = .326$, or interaction of Presentation and Session, $F(18,162) = 0.93$, $p = .542$. Thus, the ANOVA reiterated the basic result of facilitated RTs across presentations within session but found no evidence of additional changes over time.

4. fMRI results

4.1. Experience-dependent changes in activity were identified at the group and single-subject levels

The primary purpose of this experiment was to examine the pattern of PMN activity that might be observed as a result of stimulus/task repetition. This question was examined in two different ways: first, a standard whole-brain group-level analysis identified voxels exhibiting repetition-related changes (P3 > P1 or P1 > P3), after first identifying those which showed a significant Presentation x Time Point interaction (see Methods). In addition, because of the large amount of data collected per subject (30 scan runs), this same analysis was repeated at the single-subject level. Single-subject analyses were important, as PMN regions tend to be fairly limited in their areal extent (cf. Power et al., 2011), and thus may be particularly susceptible to distortions during typical group-averaging (for related discussion, see Gordon et al., 2017b). Thus, at the group level, voxels from neighboring default mode or frontoparietal regions may be averaged to varying degrees across subjects, which could potentially distort the group-level results.

Across both analysis approaches, regions exhibiting repetition-related changes in activity (both increases and decreases) were evident across much of the cortical surface (Fig. 3, Table 2, Supplementary Table 1). Indeed, these effects were consistent with those identified in a recent meta-analysis by Kim (2017) as reliably exhibiting repetition suppression and enhancement effects (i.e., reductions or increases in BOLD responses, respectively): repetition-related decreases were present across frontal and ventral visual cortex (for representative time courses, see Supplementary Fig. S2), and increases were present in regions of lateral and medial parietal cortex (the latter extending from the parieto-occipital sulcus to the cingulate gyrus).

4.2. Initial, but not final, presentations of stimuli were associated with deactivations within the PMN

Clusters exhibiting P3 > P1 activity and that were proximal to *a priori* coordinates of PMN regions were used to define ROIs (see Methods; Supplementary Fig. S3). From these, response time courses for different item Presentations could be extracted and compared to resting baseline. Although a difference between conditions was required based on the manner in which the ROIs were defined, the form of this difference remained unclear (and was verified in a subsequent analysis, as will be described later in this report). Based on prior literature, two patterns were expected: novel (P1) presentations should deactivate the PMN, whereas familiar (P3) presentations should activate PMN regions.

For the group analysis, significant deactivations from baseline were present during P1 across PMN regions (Fig. 4, blue lines). With one exception, both left and right ROIs showed significant deactivations (least significant difference: $t(9) = 4.35$, $p = .002$, obtained for the right PCU). The single ROI which failed to show significant deactivation was in the left PCU; this region exhibited numeric deactivation but did not survive multiple comparison correction ($t(9) = 2.30$, $p = .047$, Bonferroni-corrected $\alpha = 0.01$). Broadly speaking, the predicted deactivations were therefore observed for novel items, even when stimulus novelty was implicit to the actual task demands.

Results were markedly different in the group analysis of Presentation 3 (familiar item) responses (Fig. 4, red lines). These did not significantly differ from baseline in any ROI (most significant difference: $t(9) = 1.20$, $p = .258$, Bonferroni-corrected $\alpha = 0.01$; obtained for the left pIPL/dAG). Thus, whereas typically-observed deactivations were present for novel items, the task did not produce the predicted above-baseline activations for familiar items.

4.3. Subject-specific PMN ROIs also exhibit deactivation during initial presentations but not activation during final presentations

It was conceivable that the relatively small size of PMN regions and their anatomical variability resulted in repetition-related effects being missed in the group analysis. To address this concern, unsmoothed whole-brain maps were generated for each subject based on the 3 experimental runs collected across each of their 10 sessions, and the same analysis approach (a Presentation x Time Point ANOVA, followed by a Presentation 3 – Presentation 1 paired-samples, two-tailed *t*-test) was conducted for each single subject. By identifying ROIs within each subject, and averaging these values across subjects, it might be possible to

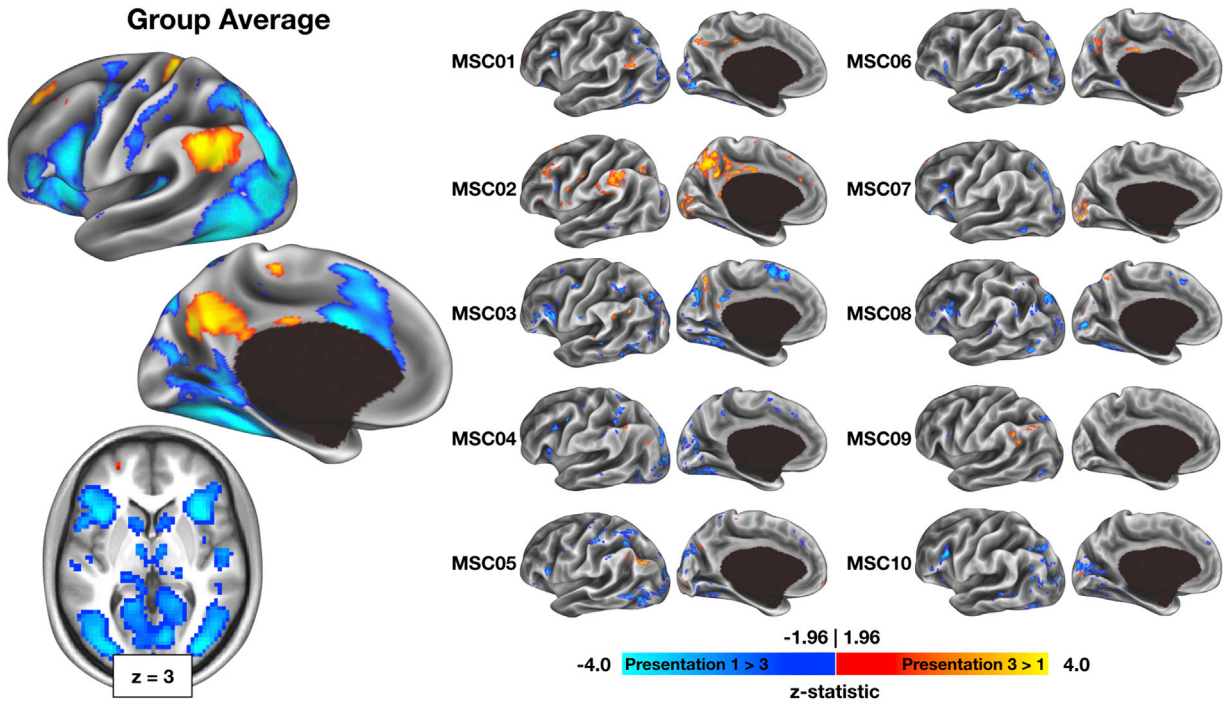

Fig. 3. Group- and subject-level contrast maps. Statistical images were generated first by conducting a Presentation (1–3) by Time Point (1–8) repeated-measures ANOVA (not shown), requiring a $z > 3$ and a voxel extent of at least 13 voxels. A paired-samples, two-tailed *t*-test (Presentation 3 – Presentation 1) in ANOVA-identified voxels then identified the directionality of repetition-related activity changes. P1 > P3 effects are presented in cool colors, and P3 > P1 effects are presented in warm colors. Statistical maps were projected onto inflated surface representations of the human brain using Connectome Workbench software (Marcus et al., 2011).

Table 2
Regions identified in the group whole-brain Presentation 3 > Presentation 1 contrast.

Region label	X	Y	Z	z-stat
R Anterior Superior Frontal Gyrus	25	61	15	1.98
R Anterior Middle Frontal Gyrus	44	61	9	3.54
L Orbitofrontal cortex	−13	60	−19	2.90
L Frontopolar Cortex	−28	56	2	2.82
L Superior Frontal Gyrus	−17	39	40	2.32
L Middle Frontal Gyrus	−29	25	46	2.45
L Middle Frontal Gyrus	−40	17	43	2.40
R Middle Frontal Gyrus	31	23	45	3.56
R Inferior Temporal Gyrus	68	2	−20	3.11
Anterior/Mid-cingulate Cortex	−1	−17	27	3.00
L Motor Cortex	−26	−27	51	3.56
L Somatomotor Cortex	−1	−28	57	2.79
Mid-cingulate Cortex	−2	−36	22	2.94
Mid-cingulate/Posterior Cingulate Cortex	−5	−44	30	3.04
L Posterior Cingulate Cortex	−14	−51	32	2.95
R Anterior Inferior Parietal Lobule	59	−51	39	2.93
R Angular Gyrus	61	−51	23	2.28
R Angular Gyrus	54	−63	28	2.22
R Angular Gyrus	45	−69	44	4.43
L Anterior Inferior Parietal Lobule	−53	−53	41	2.01
R Posterior Inferior Parietal Lobule	50	−53	46	3.26
R Posterior Inferior Parietal Lobule	47	−59	36	3.45
L Posterior Inferior Parietal Lobule	−44	−58	37	3.14
R Precuneus	9	−59	34	1.94
L Precuneus	−12	−63	34	2.56
L Dorsal Precuneus	−5	−65	45	2.06
L Angular Gyrus	−53	−65	27	2.79
L Angular Gyrus	−42	−68	47	3.25
R Cerebellum	40	−75	−28	3.43
L Cerebellum	−32	−79	−36	3.27
R Visual Cortex	18	−100	1	3.68
R Visual Cortex	20	−101	12	2.44
L Visual Cortex	−18	−102	−1	2.38

ignore possible across-region blurring (albeit with certain PMN regions absent from certain subjects' statistical maps, see Fig. 3, right).

Average responses extracted from subject-specific ROIs converged with the results of the initial group analysis (for time courses, see Supplementary Fig. S2). Significant deactivations were typically present across PMN regions (left pIPL/dAG: $t(6) = -6.40$, $p = .001$; right PCU: $t(5) = 4.58$, $p = .006$; Bonferroni-corrected $\alpha = 0.01$) during Presentation 1, and several additional regions approached significance but did not survive full Bonferroni correction (right pIPL/dAG, $t(4) = 3.82$, $p = .019$; left PCU: $t(4) = 3.07$, $p = .037$). The MCC ROI was not reliably observed in this single subject analysis and did not exhibit significant deactivation ($t(2) = 2.15$, $p = .165$). No activations (or indeed, significant perturbations from baseline) were present during Presentation 3 (most significant difference: $t(5) = 2.08$, $p = .092$, Bonferroni-corrected $\alpha = 0.01$; obtained for the right PCU. All other $ps > .54$). Thus, these data also support deactivation to initial presentation but not activation for the third presentation.

4.4. Converging results were observed within PMN ROIs defined using resting-state functional connectivity

The prior analyses suggest that only a subset of expected effects within the PMN occurred within single subjects as well as at a group level. However, ROIs were not defined independently from the data used in the one-sample *t*-tests for P1 and P3 activity. This may have biased the prior results to exaggerate deactivations or otherwise distort the underlying data. If this were true, the conclusions drawn in this study would not be valid. However, in addition to task data, the Midnight Scan Club dataset also contained a large amount (5 h) of resting-state data in each subject. We therefore turned to resting-state functional connectivity to identify PMN ROIs using data that were completely independent from those of the task, to examine deactivations (and potential activations) within PMN regions. Subject-specific PMN regions were identified using

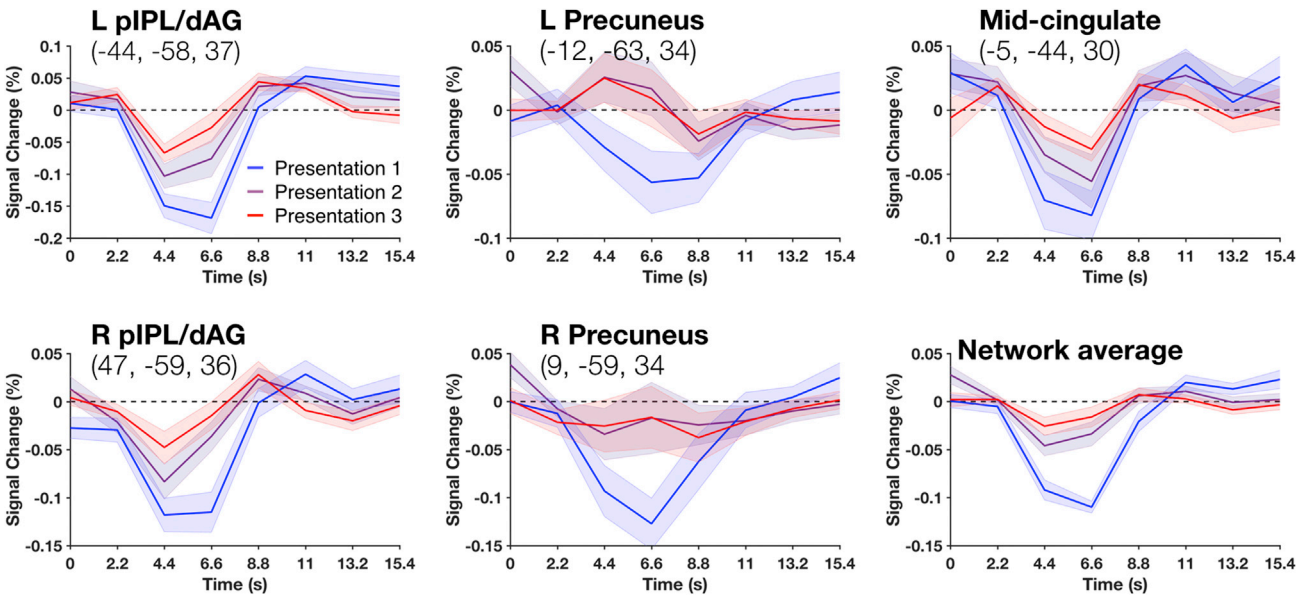

Fig. 4. BOLD response time courses for PMN regions. Regions deactivated during Presentation 1 (i.e., for novel stimuli) but did not significantly differ from baseline during Presentation 3 (for familiar stimuli). This pattern is evident for single ROIs as well as a network average. Shaded bars reflect SEM. Coordinates are in MNI152 space.

a previously-described template matching procedure (Gordon et al., 2017a), in which the correlation map for each node is assigned to an established set of network priors (Power et al., 2011) in a winner-take-all fashion. After identifying centers of mass in canonical PMN regions (see Methods), activity was averaged across subjects and used to determine if deactivations for novel, and activations for familiar, stimuli could be observed.

The network maps and corresponding response time courses for each subject are presented in Fig. 5. Results from this analysis converge with those in our prior analyses. Presentation 1 was associated with significant

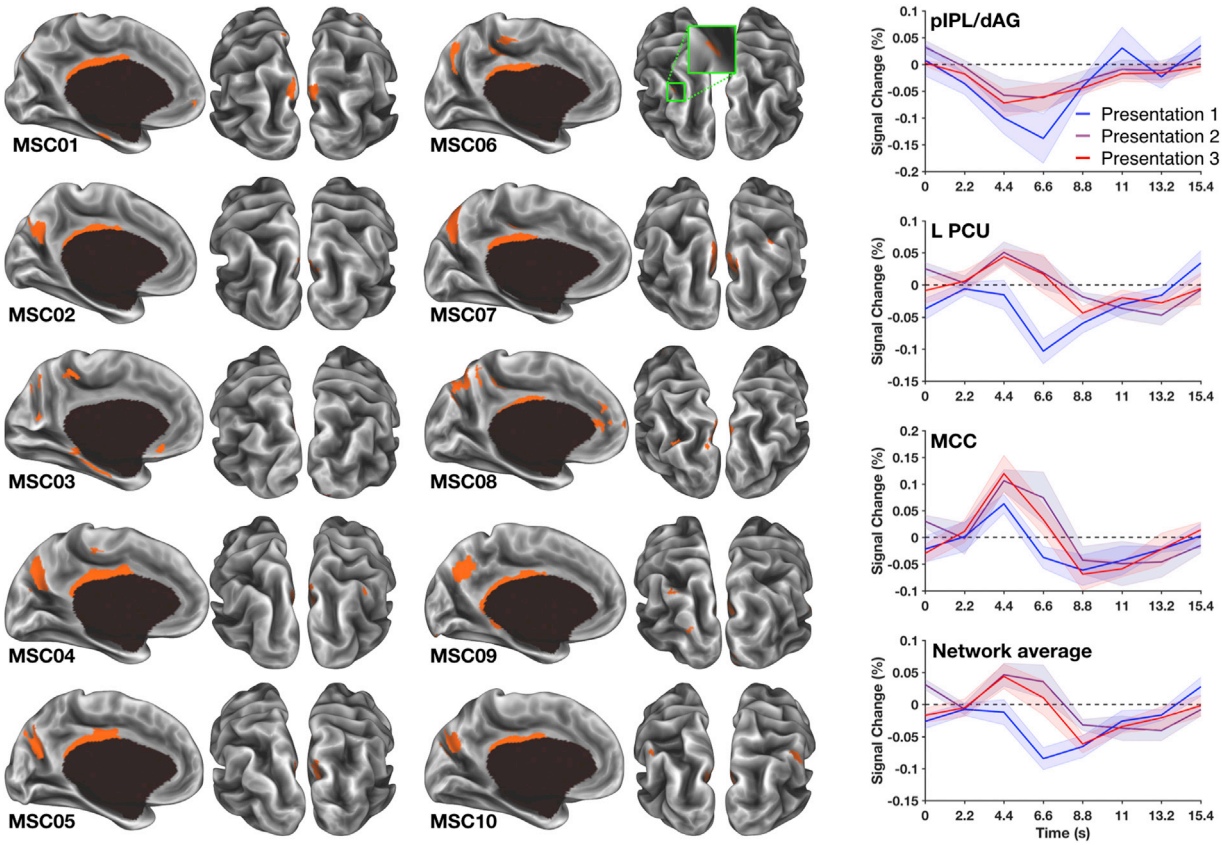

Fig. 5. Resting-state-defined networks replicate results observed in task-defined PMN regions. Left: Subject-specific PMN estimations using a previously-described template matching algorithm (Gordon et al., 2017a). Right: Time courses derived from the centers of mass of canonical PMN regions, averaged across participants. Shaded bars reflect SEM.

deactivations in pIPL and PCU regions (least significant value: $t(5) = 5.679$, $p = .002$, obtained for pIPL; Bonferroni-corrected $\alpha = 0.0125$). The exception to this was MCC, which did not significantly differ from zero, $t(9) = 0.675$, $p = .517$. Presentation 3 was not accompanied by significant activation (versus zero) in any identified regions, although in this analysis we did observe a nonsignificant tendency toward activation in MCC, $t(9) = 1.91$, $p = .088$ (Bonferroni-corrected $\alpha = 0.0125$). Thus, irrespective of how PMN regions were defined in the current study—either using task data or independent resting-state data—we observed significant perturbations in PMN region activity for novel, but never for familiar, stimuli.

To ensure that the results of the template-matching procedure generalized to other resting-state analysis approaches, we separately identified the PMN using the community detection algorithm Infomap (Rosvall and Bergstrom, 2008; Power et al., 2011). After identifying centers of mass in PMN regions (see Methods), responses to novel and familiar stimuli (P1 and P3 responses) were again compared against baseline.

The spatial topology of the PMN defined using Infomap is similar to that obtained using the template matching procedure and maps for each subject are provided in Supplementary Fig. S2, although fewer pIPL regions were identified using this approach and more anterior midline regions were associated with the network. pIPL again exhibited deactivations during initial presentation, $t(3) = 4.39$, $p = .022$, although this did not survive full Bonferroni correction. L PCU exhibited a nonsignificant tendency toward deactivation when defined using Infomap, $t(9) = 2.0$, $p = .083$. In this analysis, neither R PCU nor MCC exhibited significant deactivations relative to baseline (most significant value: $t(9) = 0.366$, $p = .723$, obtained for R PCU). As before, no PMN regions exhibited significant perturbations in response to familiar stimuli.

5. Discussion

The nature of repetition-related changes in PMN activity was examined under conditions of repeated semantic classification, without explicit retrieval demands. Previously, we posited that activity in this network primarily reflects stimulus novelty or familiarity. Under this view, one would expect the obtained BOLD response in pIPL/dAG, PCU, and MCC regions to exhibit deactivation for initial presentation and activation for the third encounter with the stimuli in the experimental task. The current work was meant to test this prediction directly within highly-sampled subjects in a task that did not rely on explicit retrieval. Although we observed deactivations in response to novel stimuli and repetition-related changes in activity, we did not observe the predicted patterns of activation for familiar stimuli. Instead, PMN responses no longer deviated significantly from baseline. The implications of these results are considered below.

5.1. On the observed repetition suppression effects

Among the most reliably-observed effects in fMRI is a reduction in evoked activity accompanying repeated exposures to a stimulus—often called repetition suppression (Raichle et al., 1994; Buckner and Koutstaal, 1998; Schacter and Buckner, 1998; Wiggs and Martin, 1998). Given the design of the present experiment, it is not surprising that such effects occurred in the lateral frontal and occipitotemporal regions with which they have previously been associated (Dobbins et al., 2004; Kim, 2017). Reductions in RT have also been associated with reductions in BOLD responses in regions near the anterior cingulate cortex and anterior insula/frontal operculum (e.g., Neta et al., 2014), and so these effects, too, are consistent with what would generally be expected in this type of design. Effects consistent with the observed P1 > P3 effects have thus been discussed at length in previous works. In this report, the focus instead is on P3 > P1 effects—specifically within the PMN—to maximize the utility of the present data.

5.2. Predicted deactivations—but not activations—are observed in PMN regions across repeated presentations

PMN deactivation in the presence of experimentally novel stimuli was both predicted and observed in this experiment. Furthermore, PMN regions appeared sensitive to stimulus history insofar as their activity patterns changed across stimulus repetitions. The obtained results were therefore consistent with several key aspects of the predictions outlined by Gilmore et al. (2015), both within single subjects and at the broader group level.

However, above-baseline activation did not occur in the PMN in response to familiar items, as had been predicted. Defining the PMN using resting-state data revealed a non-significant tendency toward activation, but this was not mirrored in task-based ROI analyses. Crucially, familiar items in this experiment were presented in the absence of an explicit retrieval task and were blocked with stimuli of similar item histories—both departures from typical fMRI memory task designs. Thus, we consider two possible explanations for this outcome: either participants did not consider stimuli to be subjectively familiar by their third presentation (which seems unlikely, and was contradicted by informal subject debriefings), or information processing within the PMN operates such that no activations were present *despite* the familiarity of the Presentation 3 stimuli (which we argue is theoretically more interesting). These results suggest that several aspects of the original novelty/familiarity hypothesis need to be updated and tested in future work.

First, the present findings demonstrate that task-relevance plays a significant role in PMN responses to familiar items, echoing similar conclusions by Rosen et al. (2017), Gilmore et al. (2019). This observation stands in contrast to the novelty-related deactivations, which were observed both in the current dataset as well as in "initial study" periods of prior experiments (e.g., Vannini et al., 2011). These deactivations might therefore be considered bottom-up in nature (we discuss further implications of this possibility below). Familiarity-related responses within the PMN have been modulated by attentional manipulations in other recent experiments, as well. One recent series of experiments examined the functional-anatomic correlates of memory-guided direction of visuospatial attention (Rosen et al. 2016, 2017). Rosen et al. found that regions corresponding to those within the PMN were maximally activated when attention was guided by episodic memory retrieval, above and beyond activity that was elicited in the presence of familiar stimuli without additional attentional requirements. Work by Gilmore et al. (2019) found that Familiar > Novel effects exist in PMN regions across task conditions but found overall greater activity during explicit retrieval than a repeated object naming condition. It is notable that the regions associated with novelty and familiarity during object naming in that report were similar to those observed here. In yet other work, manipulations that affected the *expectation* of stimulus familiarity were found to modify activity within the pIPL/dAG (O'Connor et al., 2010; Jaeger et al., 2013), with more unexpected outcomes being associated with greater activity (but see Herron et al., 2004). These previous studies—taken together with the present results—indicate that activity within PMN regions may be maximally evoked when familiarity is both present and the locus of one's attention.

5.3. Are there multiple forms of repetition enhancement within the PMN?

Gilmore et al. (2015) described the shift from novelty-related deactivation to familiarity-related activation as a form of repetition enhancement that occurred along a continuum. However, in the present work, no significant above-baseline activation was observed, even during Presentation 3 periods. One question raised by the outcome of the current experiment relates to whether the repetition-related changes in activity may be comprised of two dissociable components: novel to no-longer--novel—signaled initially by deactivation and a subsequent lack of deactivation—and less familiar to increasingly-familiar—signaled by activation to varying degrees. Broadly speaking, such a distinction would be consistent with prior suggestions that novelty and familiarity

detection may reflect distinct processes (Habib et al., 2003; Daselaar et al., 2006; Kafkas and Montaldi, 2014, 2018; Rutishauser et al., 2015). It would also imply that the "novelty-familiarity" dimension previously associated with activity within the PMN may instead represent two separate dimensions. Such a separation is consistent with the possibility that novelty-related deactivations within the PMN may be less sensitive to changes in task demand than are the familiarity-related signals. This conclusion would also be consistent with the results discussed in Section 5.2 (e.g., O'Connor et al., 2010; Jaeger et al., 2013), as they primarily focused on task-related perturbations of familiar items.

Considering novelty-related processing and familiarity-related processing as separate phenomena allows us to make sense of our observations in the context of the wide literature on repetition suppression. In particular, models built to explain effects related to repetition suppression (e.g., Wiggs and Martin, 1998; Friston, 2005; Gotts et al., 2012) might prove equally useful if applied to situations in which reductions in *deactivation* (rather than activation) are associated with changes in activity across multiple stimulus presentations. Under this view, the repetition-related changes presently observed under blocked presentation conditions may not constitute a processing of familiarity in the same manner above-baseline activations have been interpreted in previous work (Gilmore et al., 2015). Rather, decreases in deactivation might reflect a reduced overall perturbation of PMN regions in the absence of explicit memory task demands much in the same way as in processing regions such as IFG or ventral occipitotemporal cortex. If novelty-related effects are reduced or eliminated through a type of "sharpening" or Bayesian prediction model, then this would result in a suppression of negative BOLD responses in PMN regions that would coincide with activation brought on by task-relevant familiarity. Importantly, this possibility would be consistent with separate processing of novelty and familiarity dimensions within the PMN. This possibility—highlighted in the current data—should be examined further in future work.

5.4. Laterality of the PMN

In the initial characterization of the PMN, the question was raised whether the PMN was left-lateralized or was present in both hemispheres (Gilmore et al., 2015). Meta-analyses of task data generally suggested the former, whereas resting-state analyses suggested the latter. Over the past several years, converging evidence appears to support bilaterality of the PMN.

In the current experiment, PMN ROIs were frequently identified in both hemispheres (Figs. 3 and 5). This was true for the group as well as for single subjects. In addition, other recent task-evoked fMRI results have suggested bilaterality within the PMN. For example, Chen et al. (2017) recently found familiarity-related activity differences in pIPL/dAG and PCU bilaterally in a task comparing autobiographical and recognition memory retrieval. McDermott et al. (2017) also observed bilateral activations in a DRM recognition memory test (Roediger and McDermott, 1995), both for stimuli that were objectively familiar (hits) as well as those which were incorrectly recognized (false alarms). Within the domain of spatial navigation, Brodt et al. (2016) found that bilateral midline PMN regions continued to exhibit repetition enhancement effects for up to 60 item repetitions (the experimental maximum) if the items were placed statically in the maze.

An alternative account was recently proposed by Rosen et al. (2017), who proposed that the PMN was a left-lateralized portion of a larger "Memory-Attention Network," which would consist of PMN regions in both hemispheres as well as bilateral portions of the cerebellum, thalamus, and striatum. Although intriguing, the proposed Memory-Attention Network has not been isolated as a distinct network in other studies that have identified functional network communities, including those that have examined cerebellar and subcortical regions (e.g., Buckner et al., 2011; Greene et al., 2014; Hwang et al., 2017). Furthermore, to the extent that we observed any repetition-related effects in subcortical structures within the MSC data, they were overwhelmingly in the opposite direction of those observed within the PMN (Fig. 3, Supplemental Table 1). Consequently, we argue that the balance of evidence suggests a bilateral PMN, and we suggest that the Memory-Attention Network as described by Rosen et al. may have been a result of task-related regional co-activation.

5.5. Inter-subject variability in PMN regions

Three regions have previously been associated with the PMN: the pIPL/dAG, PCU, and MCC. At the group level, we continued to observe this within our cohort of subjects. However, at the single-subject level, we observed appreciable variability. Relatively few subjects displayed expected patterns of activity in all putative PMN regions during the task (Fig. 3) or in an independent analysis of resting-state data (Fig. 5), and region locations varied across subjects in a manner that would not necessarily be anticipated from the group-level analysis. That is, at the group level, the observed P3 > P1 map recapitulated many aspects of the default mode network (Fig. 3; cf. Buckner et al., 2008), but this differed substantially from the individual-level maps, which appeared both sparser and more consistent with the PMN as previously described (cf. Gilmore et al., 2015; McDermott et al., 2017). This may have been a result of the relatively small size of our group (N = 10), and the presence of sub-threshold effects that did not emerge at the thresholds used in the single-subject analyses.

We also found that a clear pIPL/dAG region was absent from several subjects' network maps, or it was only located on a single hemisphere (Fig. 5, Supplemental Fig. S5). This variability was presaged in recent work by Gordon et al. (2017a), was described separately within the current subjects in Gordon et al. (2017b), and is consistent with prior reports of variability in lateral parietal cortex (Mueller et al., 2013; Laumann et al., 2015). In addition, certain previous analyses, such as the 17-network solution reported by Yeo et al. (2011), identified only PCU and MCC components as falling within the same network community, with the pIPL/dAG falling in a separate community. Collectively, these results suggest variability in connectivity of pIPL/dAG regions (and lateral parietal regions more broadly) across different individuals. The degree to which an individual's behavior may be impacted by the presence, location, or size of different PMN regions is presently unclear (as it is with other functional networks) and will need to be answered in future experiments with substantially larger sample sizes.

5.6. Limitations and future directions

As with any single experiment, design limitations narrow the interpretation of obtained results. We now consider several routes forward in future experiments that may support and extend the findings discussed in this report.

5.6.1. Are the current findings a result of the "blocked" order of stimulus presentation?

In each run, all stimuli were observed a single time before being observed a second time, and all were seen twice before any were seen a third time. A benefit of this design is that the initial presentation blocks are comparable to initial encoding blocks used in numerous fMRI studies (and, indeed, we observed deactivations in "posteromedial" cortex, as would be expected from prior literature). However, the current study departs from many designs in that it does not then intermix novel and familiar stimuli during a subsequent test phase. Instead, all items within a presentation block share a common history (barring transition points from Presentation 1 to Presentation 2, or 2 to 3). This design choice has implications for interpretation of both behavioral and fMRI results described in this report. First, although faster response times are consistent with—and likely attributable to—repetition priming (that is, response facilitation as a result of recent prior exposure with the same stimuli and same semantic judgments; see e.g., Dobbins et al., 2004; Schacter et al., 2004; Saggar et al., 2010), it is possible that the RT improvements across presentations could have been demonstrated even for

novel items, had they been interposed between familiar stimuli. The observation that no session-to-session RT facilitation was observed seems to argue against this type of "generalized learning" account, but it does not rule out the possibility that within-session improvements may have at least partly reflected some form of practice effect.

With respect to the obtained fMRI results, the blocked nature of the stimuli may have reduced the salience of familiarity-related information, and thus reduced neural activity associated with the familiarity. This explanation allows for several clear predictions: under rapidly-presented incidental encoding conditions (as was done here), blocked novel stimuli should produce deactivations (relative to rest) within the PMN; blocked familiar stimuli should not produce significant perturbations (replicating the results observed here); and intermixed novel and familiar stimuli should elicit significant above-baseline activation for familiar stimuli. Intermixing novel and familiar stimuli and alternating between different task states should increase neural responses within the PMN, thereby creating a situation in which the PMN might be better differentiated from adjacent DMN regions that appear to behave similarly under the current experimental conditions (see Gilmore et al., 2019).

5.6.2. Understanding the dynamic range of responses in PMN regions

Based on the persistence of deactivations—but not activations—in the current dataset, a logical question is whether the deactivations and activations are supported by the same or different neuronal populations. It may be the case that the cells within PMN regions responding to novelty are distinct from those that respond to familiarity, or it may be the case that the same populations respond to both as others have observed (Rutishauser et al. 2015, 2017). Identifying which possibility is correct has important implications for understanding information processing within the PMN: in the former case there are distinct signals being processed for novelty and familiarity, whereas in the latter case it may be more appropriate to characterize novelty and familiarity as being along a single continuum. The answer to this question likely lies outside the realm of fMRI (presumably involving intracranial recording) but could have profound implications for the broader question of how novelty and familiarity may relate to one another.

5.6.3. Further improvements in functional-neuroanatomic mapping

The use of small-N, high-data designs has the benefit of avoiding the across-subject anatomical blurring that has characterized much of the fMRI literature (e.g., Gordon et al., 2017b; Marek et al., 2018). In the current experiment, both the group-level and individual-level analysis streams provided convergent results. However, the dataset used here was not collected using a high-resolution scan sequence, and thus the voxel sizes were larger than they might otherwise have been. Just as we have attempted to isolate specific cortical regions within the current data, further improvements in within-subject resolution may provide additional certainty regarding the locations and extents of parcels within parietal cortex and beyond.

6. Conclusions

In the present experiment, a semantic decision task was used to assess PMN activity when stimuli were encountered repeatedly within a semantic decision task, using a group of highly-sampled subjects. Results suggest that the activations observed in previous experiments were likely attributable to specific task demands more than simple familiarity *per se*. This provides an important boundary condition for the "flip" that was recently described as a core characteristic of the PMN (Gilmore et al., 2015) and suggests that task conditions play a larger role than was previously appreciated in retrieval-related network activity.

Acknowledgements

We thank Ian Dobbins, Roddy Roediger, Ben Seitzman, Avi Snyder, and members of the Memory and Cognition lab at Washington University for helpful discussions. We also thank Liam Comiskey, Andrew Fishell, and Rashina Seabury for assistance with data collection.

This work was supported by a National Science Foundation Graduate Research Fellowship DGE-1143954 (AWG); National Institutes of Health Grants NS088590, TR000448 (NUFD), MH104592 (DJG), 1R25MH112473 (TOL), 1P30NS098577 (to the Neuroimaging Informatics and Analysis Center), and HD087011 (to the Intellectual and Developmental Disabilities Research Center at Washington University); the Jacobs Foundation (NUFD); the Child Neurology Foundation (NUFD); the McDonnell Center for Systems Neuroscience (NUFD, BLS); the Mallinckrodt Institute of Radiology (NUFD); the Hope Center for Neurological Disorders (NUFD, BLS, SEP); an American Psychological Association dissertation research award (AWG) and Dart Neuroscience, LLC (KBM).

Appendix A. Supplementary data

Supplementary data to this article can be found online at https://doi.org/10.1016/j.neuroimage.2019.06.011.

References

Balota, D.A., Yap, M.J., Corsese, M.J., Hutchison, K.A., Kessler, B., Loftis, B., Neely, J.H., Nelson, D.L., Simpson, G.B., Trieman, R., 2007. The English lexicon project. Behav. Res. Methods 39, 445–459.

Ben-Zvi, S., Soroker, N., Levy, D.A., 2015. Parietal lesion effects on cued recall following pair associate learning. Neuropsychologia 73, 176–194.

Berryhill, M.E., 2012. Insights from neuropsychology: pinpointing the role of the posterior parietal cortex in episodic and working memory. Front. Integr. Neurosci. 6, 1–12.

Berryhill, M.E., Phuong, L., Picasso, L., Cabeza, R., Olson, I.R., 2007. Parietal lobe and episodic memory: bilateral damage causes impaired free recall of autobiographical memories. J. Neurosci. 27, 14415–14423.

Braga, R.M., Buckner, R.L., 2017. Parallel interdigitated distributed networks within the individual estimated by intrinsic functional connectivity. Neuron 95, 457–471.

Brodt, S., Pöhlchen, D., Flanagin, V.L., Glasauer, S., Gais, S., Schönauer, M., 2016. Rapid and independent memory formation in the parietal cortex. Proc. Natl. Acad. Sci. U.S.A. 113, 13251–13256.

Buckner, R.L., Andrews-Hanna, J.R., Schacter, D.L., 2008. The brain's default network: anatomy, function, and relevance to disease. Ann. N. Y. Acad. Sci. 1124, 1–38.

Buckner, R.L., Koutstaal, W., 1998. Functional neuroimaging studies of encoding, priming, and explicit memory retrieval. Proc. Natl. Acad. Sci. U.S.A. 95, 891.

Buckner, R.L., Krienen, F.M., Castellanos, A., Diaz, J.C., Yeo, B.T.T., 2011. The organization of the human cerebellum estimated by intrinsic functional connectivity. J. Neurophysiol. 106, 2322–2345.

Bzdok, D., Heeger, A., Langner, R., Laird, A.R., Fox, P.T., Palomero-Gallagher, N., Vogt, B.A., Zilles, K., Eickhoff, S.B., 2015. Subspecialization in the human posterior medial cortex. Neuroimage 106, 55–71.

Cabeza, R., Ciaramelli, E., Moscovitch, M., 2012. Response to Nelson et al.: ventral parietal subdivisions are not incompatible with an overarching function. Trends Cognit. Sci. 16, 400–401.

Chen, H.-Y., Gilmore, A.W., Nelson, S.M., McDermott, K.B., 2017. Are there multiple kinds of episodic memory? An fMRI investigation comparing autobiographical and recognition memory tasks. J. Neurosci. 37, 2764–2775.

Ciaramelli, E., Grady, C.L., Moscovitch, M., 2008. Top-down and bottom-up attention to memory: a hypothesis (AtoM) on the role of the posterior parietal cortex in memory retrieval. Neuropsychologia 46, 1828–1851.

Cohen, J.D., MacWhinney, B., Flatt, M., Provost, J., 1993. PsyScope: a new graphic interactive environment for designing psychology experiments. Behav. Res. Methods Instrum. Comput. 25, 257–271.

Dale, A.M., Fischl, B., Sereno, M.I., 1999. Cortical surface-based analysis. I: segmentation and surface reconstruction. Neuroimage 9, 179–194.

Daselaar, S.M., Fleck, M.S., Cabeza, R., 2006. Triple dissociation in the medial temporal lobes: recollection, familiarity, and novelty. J. Neurophysiol. 96, 1902–1911.

Davidson, P.S.R., Anaki, D., Ciaramelli, E., Cohn, M., Kim, A.S.N., Murphy, K.J., Troyer, A.K., Moscovitch, M., Levine, B., 2008. Does lateral parietal cortex support episodic memory? Evidence from focal lesion patients. Neuropsychologia 46, 1743–1755.

Dobbins, I.G., Schnyer, D.M., Verfaellie, M., Schacter, D.L., 2004. Cortical activity reductions during repetition priming can result from rapid response learning. Nature 428, 316–319.

Doucet, G., Naveau, M., Petit, L., Delcroix, N., Zago, L., Crivello, F., Jobard, G., Tzourio-Mazoyer, N., Mazyoer, B., Mellet, E., Joliot, M., 2011. Brain activity at rest: a multiscale heirarchical functional organization. J. Neurophysiol. 105, 2753–2763.

Elman, J.A., Shimamura, A.P., 2011. Task relevance modulates successful retrieval effects during explicit and implicit memory tests. Neuroimage 56, 345–353.

Fischl, B., Sereno, M.I., Dale, A.M., 1999. Cortical surface-based analysis. II: inflation, flattening, and a surface-based coordinate system. Neuroimage 9, 195–207.

Friston, K., Jezzard, P., Turner, R., 1994. Analysis of functiona MRI time-series. Hum. Brain Mapp. 1, 153–171.

Friston, K.J., 2005. A theory of cortical responses. Phil Trans R Soc B 360, 815–836.

Friston, K.J., Williams, S., Howard, R., Frackowiak, R.S.J., Turner, R., 1996. Movement-related effects in fMRI time-series. Magn. Reson. Med. 35, 346–355.
Gilmore, A.W., Kalinowski, S.E., Milleville, S.C., Gotts, S.J., Martin, A., 2019. Identifying task-general effects of stimulus familiarity in the parietal memory network. Neuropsychologia 124, 31–43.
Gilmore, A.W., Nelson, S.M., McDermott, K.B., 2015. A parietal memory network revealed by multiple MRI methods. Trends Cognit. Sci. 19, 534–543.
Glasser, M.F., Sotiropoulos, S.N., Wilson, J.A., Coalson, T., Fischl, B., Andersson, J.L., Xu, J., Jbadbi, S., Webster, M., Polimeni, J.R., Van Essen, D.C., Jenkinson, M., Consortium ftW, M.H., 2013. The minimal preprocessing pipelines for the Human Connectome Project. Neuroimage 80, 105–124.
Gordon, E.M., Laumann, T.O., Adeyemo, B., Gilmore, A.W., Nelson, S.M., Dosenbach, N.U.F., Petersen, S.E., 2017a. Individual-specific features of brain systems identified with resting state functional correlations. Neuroimage 146, 918–939.
Gordon, E.M., Laumann, T.O., Gilmore, A.W., Newbold, D.J., Greene, D.J., Berg, J.J., Ortega, M., Hoyt-Drazen, C., Gratton, C., Sun, H., Hampton, J.M., Coalson, R.S., Nguyen, A.L., McDermott, K.B., Shimony, J.S., Snyder, A.Z., Schlaggar, B.L., Petersen, S.E., Nelson, S.M., Dosenbach, N.U.F., 2017b. Precision functional mapping of individual human brains. Neuron 95, 791–807 e797.
Gotts, S.J., Chow, C.C., Martin, A., 2012. Repetition priming and repetition suppression: a case for enhanced efficiency through neural synchronization. Cogn. Neurosci. 3, 227–237.
Gratton, C., Laumann, T., Nielsen, A.N., Greene, D.J., Gordon, E.M., Gilmore, A.W., Nelson, S.M., Coalson, R.S., Snyder, A.Z., Schlaggar, B.L., Dosenbach, N.U.F., Petersen, S.E., 2018. Functional brain networks are dominated by stable group and individual factors, not cognitive or daily variation. Neuron 98, 439–452 e435.
Greene, D.J., Laumann, T.O., Dubis, J.W., Ihnen, S.K., Neta, M., Power, J.D., Pruett Jr., J.R., Black, K.J., Schlaggar, B.L., 2014. Developmental changes in the organization of functional connections between basal ganglia and cerebral cortex. J. Neurosci. 34, 5842–5854.
Habib, R., McIntosh, A.R., Wheeler, M.A., Tulving, E., 2003. Memory encoding and hippocampally-based novelty/familiarity discrimination networks. Neuropsychologia 41, 271–279.
Herron, J.E., Henson, R.N.A., Rugg, M.D., 2004. Probability effects on the neural correlates of retrieval success: an fMRI study. Neuroimage 21, 302–310.
Hond, D., Spacek, Leditors, 1997. Distinctive descriptions for face processing. In: Proceedings of the 8th British Machine Vision Conference BMVC97; 1997 September. Colchester, England, pp. 320–329.
Huijbers, W., Schultz, A.P., Vannini, P., McLaren, D.G., Wigman, S.E., Ward, A.M., Hedden, T., Sperling, R.A., 2013. The encoding/retrieval flip: interactions between memory performance and memory stage and relationship to intrinsic functional networks. J. Cogn. Neurosci. 25, 1163–1179.
Hwang, K., Bertolero, M.A., Liu, W.B., D'Esposito, M., 2017. The human thalamus is an integrative hub for functional brain networks. J. Neurosci. 37, 5594–5607.
Jaeger, A., Konkel, A., Dobbins, I.G., 2013. Unexpected novelty and familiarity orienting respones in lateral parietal cortex during recognition judgment. Neuropsychologia 51, 1061–1076.
Kafkas, A., Montaldi, D., 2014. Two separate, but interacting, neural systems for familiarity and novelty detection: a dual-route mechanism. Hippocampus 24, 516–527.
Kafkas, A., Montaldi, D., 2018. How Do Memory Systems Detect and Respond to Novelty'. Neuroscience Letters Advanced online publication.
Kim, H., 2013. Differential neural activity in the recognition of old versus new events: an activation likelihood estimation meta-analysis. Hum. Brain Mapp. 34, 814–836.
Kim, H., 2017. Brain regions that show repetition suppression and enhancement: a meta-analysis of 137 neuroimaging experiments. Hum. Brain Mapp. 38, 1894–1913.
Kriegeskorte, N., Simmons, W.K., Bellgowan, P.S.F., Baker, C.I., 2009. Circular analysis in systems neuroscience: the dangers of double dipping. Nat. Neurosci. 12, 535–540.
Laumann, T.O., Gordon, E.M., Adeyemo, B., Snyder, A.Z., Joo, S.J., Chen, M.Y., Gilmore, A.W., McDermott, K.B., Nelson, S.M., Dosenbach, N.U.F., Schlaggar, B.L., Mumford, J.A., Poldrack, R.A., Petersen, S.E., 2015. Functional system and areal organization of a highly sampled individual human brain. Neuron 87, 657–670.
Laumann, T.O., Snyder, A.Z., Mitra, A.M., Gordon, E.M., Gratton, C., Adeyemo, B., Gilmore, A.W., Nelson, S.M., Berg, J.J., Greene, D.J., McCarthy, J.E., Schlaggar, B.L., Dosenbach, N.U.F., Petersen, S.E., 2016. On the Stability of BOLD fMRI Correlations. Cereb Cortex Advance online publication.
Lund, K., Burgess, C., 1996. Producing high-dimensional semantic spaces from lexical co-occurrence. Behav. Res. Methods Instrum. Comput. 28, 203–208.
Marcus, D.S., Harwell, J., Olsen, T., Hodge, M., Glasser, M.F., Prior, F., Jenkinson, M., Laumann, T., Curtiss, S.W., Van Essen, D.C., 2011. Informatics and data mining: tools and strategies for the human connectome project. Front. Neuroinf. 5, 4.
Marek, S., Siegel, J.S., Gordon, E.M., Raut, R.V., Gratton, C., Newbold, D.J., Ortega, M., Laumann, T.O., Adeyemo, B., Miller, D.B., Zheng, A., Lopez, K.C., Berg, J.J., Coalson, R.S., Nguyen, A., Dierker, D., Van, A.N., Hoyt, C.R., McDermott, K.B., Norris, S.A., Shimony, J.S., Snyder, A.Z., Nelson, S.M., Barch, D.M., Schlaggar, B.L., Raichle, M.E., Petersen, S.E., Greene, D.J., Dosenbach, N.U.F., 2018. Spatial and temporal organization of the individual human cerebellum. Neuron 100, 977–993 e977.
McAvoy, M.P., Ollinger, J.M., Buckner, R.L., 2001. Cluster size thresholds for assessment of significant activation in fMRI. Neuroimage 13, 198.
McDermott, K.B., Buckner, R.L., Petersen, S.E., Kelley, W.M., Sanders, A.L., 1999. Set- and code-specific activation in the frontal cortex: an fMRI study of encoding and retrieval of faces and words. J. Cogn. Neurosci. 11, 631–640.
McDermott, K.B., Gilmore, A.W., Nelson, S.M., Watson, J.M., Ojemann, J.G., 2017. The parietal memory network activates similarly for true and associative false recognition elicited via the DRM procedure. Cortex 87, 96–107.
McDermott, K.B., Szpunar, K.K., Christ, S.E., 2009. Laboratory-based and autobiographical retrieval tasks differ substantially in their neural substrates. Neuropsychologia 47, 2290–2298.
Miezin, F.M., Maccotta, L., Ollinger, J.M., Petersen, S.E., Buckner, R.L., 2000. Characterizing the hemodynamic response: effects of presentation rate, sampling procedure, and the possibility of ordering brain activity based on relative timing. Neuroimage 11, 735–759.
Mueller, S., Wang, D., Fox, M.D., Yeo, B.T.T., Sepulcre, J., Sabuncu, M.R., Shafee, R., Lu, J., Liu, H., 2013. Individual variability in functional connectivity architecture of the human brain. Neuron 77, 586–595.
Mugler III, J.P., Brookerman, J.R., 1990. Three-dimensional magnetization-prepared rapid gradient-echo imaging (3D MP RAGE). Magn. Reson. Med. 15, 152–157.
Nelson, S.M., Arnold, K.M., Gilmore, A.W., McDermott, K.B., 2013a. Neural signatures of test-potentiated learning in parietal cortex. J. Neurosci. 33, 11754–11762.
Nelson, S.M., Cohen, A.L., Power, J.D., Wig, G.S., Miezin, F.M., Wheeler, M.E., Velanova, K., Donaldson, D.I., Phillips, J.S., Schlaggar, B.L., Petersen, S.E., 2010. A parcellation scheme for human left lateral parietal cortex. Neuron 67, 156–170.
Nelson, S.M., McDermott, K.B., Petersen, S.E., 2012. In favor of a 'fractionation' view of ventral parietal cortex: comment on Cabeza et al. Trends Cognit. Sci. 16, 399–400.
Nelson, S.M., McDermott, K.B., Wig, G.S., Schlaggar, B.L., Petersen, S.E., 2013b. The critical roles of localization and physiology for understanding parietal contributions to memory retrieval. Neuroscientist 19, 578–591.
Neta, M., Schlaggar, B.L., Petersen, S.E., 2014. Separable responses to error, ambiguity, and reaction time in cingulo-opercular task control regions. Neuroimage 99, 59–68.
O'Connor, A.R., Han, S., Dobbins, I.G., 2010. The inferior parietal lobule and recognition memory: expectancy violation or successful retrieval? J. Neurosci. 30, 2924–2934.
Ojemann, J.G., Akbudak, E., Snyder, A.Z., McKinstry, R.C., Raichle, M.E., Conturo, T.E., 1997. Anatomic localization and quantitative analysis of gradient refocused echo-planar fMRI susceptibility artifacts. Neuroimage 6, 156–167.
Ollinger, J.M., Corbetta, M., Shulman, G.L., 2001a. Separating processes within a trial in event-related functional MRI II. Analysis. Neuroimage 13, 218–229.
Ollinger, J.M., Shulman, G.L., Corbetta, M., 2001b. Separating processes within a trial in event-related functional MRI I. The method. Neuroimage 13, 210–217.
Olson, I.R., Berryhill, M., 2009. Some surprising findings on the involvement of the parietal lobe in human memory. Neurobiol. Learn. Mem. 91, 155–195.
Poldrack, R.A., Barch, D.M., Mitchell, J., Wager, T.D., Wagner, A.D., Devlin, J.T., Cumba, C., Koyejo, O., Milham, M.P., 2013. Toward open sharing of task-based fMRI data: the OpenfMRI project. Front. Neuroinf. 7 dx.doi.org/10.3389/fninf.2013.00012.
Power, J.D., Cohen, A.L., Nelson, S.M., Wig, G.S., Barnes, K.A., Church, J.A., Vogel, A.C., Laumann, T.O., Miezin, F.M., Schlaggar, B.L., Petersen, S.E., 2011. Functional network organization of the human brain. Neuron 72, 665–678.
Power, J.D., Mitra, A., Laumann, T.O., Snyder, A.Z., Schlaggar, B.L., Petersen, S.E., 2014a. Methods to detect, characterize, and remove motion artifact in resting state fMRI. Neuroimage 84, 320–341.
Power, J.D., Schlaggar, B.L., Petersen, S.E., 2014b. Studying brain organization via spontaneous fMRI signal. Neuron 84, 681–696.
Raichle, M.E., Fiez, J.A., Videen, T.O., MacLeod, A.-M.K., Pardo, J.V., Fox, P.T., Petersen, S.E., 1994. Practice-related changes in human brain functional neuroanatomy during nonmotor learning. Cerebr. Cortex 4, 8–26.
Righi, G., Peissig, J.J., Tarr, M.J., 2012. Recognizing disguised faces. Vis. Cognit. 20, 143–169.
Roediger, H.L., McDermott, K.B., 1995. Creating false memories: remembering words not presented in lists. J. Exp. Psychol. Learn. Mem. Cogn. 21, 803–814.
Rosen, M.L., Stern, C.E., Devaney, K.J., Somers, D.C., 2017. Cortical and Subcortical Cotributions to Long-Term Memory-Guided Visuospatial Attention. Cereb Cortex Advanced online publication.
Rosen, M.L., Stern, C.E., Michalka, S.W., Devaney, K.J., Somers, D.C., 2016. Cognitive control network contributions to memory-guided visual attention. Cerebr. Cortex 26, 2059–2073.
Rosvall, M., Bergstrom, C.T., 2008. Maps of random walks on complex networks reveal community structure. Proc. Natl. Acad. Sci. U.S.A. 15, 1118–1123.
Rugg, M.D., King, D.R., 2017. Ventral Lateral Parietal Cortex and Episodic Memory Retrieval. Cortex Advanced online publication.
Rutishauser, U., Aflalo, T., R RE, Pouratian, N., Anderson, R.A., 2017. Single-neuron representation of memory strength and recognition confidence in left human posterior parietal cortex. Neuron 97, 1–12.
Rutishauser, U., Ye, S., Koroma, M., Tudusciuc, O., Ross, I.B., Chung, J.M., Mamelak, A.N., 2015. Representation of retrieval confidence by single neurons in the human medial temporal lobe. Nat. Neurosci. 18, 1041–1050.
Saggar, M., Miikkulainen, R., Schnyer, D.M., 2010. Behavioral, neuroimaging, and computational evidence for perceptual caching in repetition priming. Brain Res. 1315, 75–91.
Schacter, D.L., Buckner, R.L., 1998. Priming and the brain. Neuron 20, 185–195.
Schacter, D.L., Dobbins, I.G., Schnyer, D.M., 2004. Specificity of priming: a cognitive neuroscience perspective. Nat. Rev. Neurosci. 5, 853–862.
Seghier, M.L., 2013. The angular gyrus: multiple functions and multiple subdivisions. Neuroscientist 19, 43–61.
Segonne, F., Dale, A.M., Busa, E., Glessner, M., Salat, D., Hahn, H.K., Fischl, B., 2004. A hybrid approach to the skull stripping problem in MRI. Neuroimage 22, 1060–1075.
Sestieri, C., Shulman, G.L., Corbetta, M., 2017. The contribution of the human posterior parietal cortex to episodic memory. Nat. Rev. Neurosci. 18, 183–192.
Smith, S.M., Jenkinson, M., Woolrich, M.W., Beckmann, C.F., Behrens, T.E.J., Johansen-Berg, H., Bannister, P.R., De Luca, M., Drobnjak, I., Flitney, D.E., Naizy, R.K., Saunders, J., Vickers, J., Zhang, Y., De Stefano, N., Brady, J.M., Matthews, P.M., 2004. Advances in functional and structural MR image analysis and implementation as FSL. Neuroimage 23, S208–S219.

Snyder, A.Z., 1996. Difference image vs. ratio image error function forms in PET-PET realignment. In: Myer, R., Cunningham, V.J., Bailey, D.L., Jones, T. (Eds.), Quantification of Brain Function Using PET. Academic Press, San Diego, CA, pp. 131–137.
Spaniol, J., Davidson, P.S.R., Kim, A.S.N., Han, H., Moscovitch, M., Grady, C.L., 2009. Event-related fMRI studies of episodic encoding and retrieval: meta-analyses using activation likelihood estimation. Neuropsychologia 47, 1765–1779.
Tulving, E., Kapur, S., Markowitsch, H.J., Craik, F.I.M., Habib, R., Houle, S., 1994. Neuroanatomical correlates of retrieval in episodic memory: auditory sentence recognition. Proc. Natl. Acad. Sci. U.S.A. 91, 2012–2015.
Van Essen, D.C., Drury, H.A., Dickson, J., Harwell, J., Hanlon, D., Anderson, C.H., 2001. An integrated software suite for surface-based analyses of cerebral cortex. J. Am. Med. Inform. Assoc. : JAMIA 8, 443–459.
Van Essen, D.C., Glasser, M., Dierker, D., Harwell, J., Coalson, T., 2012. Parcellations and hemispheric asymmetries of human cerebral cortex analyzed on surface-based atlases. Cerebr. Cortex 22, 2241–2262.
Vannini, P., O'Brien, J., O'Keefe, K., Pihlajamaki, M., LaViolette, P.S., Sperling, R.A., 2011. What goes down must come up: role of the postermedial cortices in encoding and retrieval. Cerebr. Cortex 21, 22–34.
Vilberg, K.L., Rugg, M.D., 2008. Memory retrieval and the parietal cortex: a review of evidence from a dual-process perspective. Neuropsychologia 46, 1787–1799.
Vul, E., Pashler, H., 2012. Voodoo and circularity errors. Neuroimage 62, 945–948.
Wagner, A.D., Shannon, B.J., Kahn, I., Buckner, R.L., 2005. Parietal lobe contributions to episodic memory retrieval. Trends Cognit. Sci. 9, 445–453.
Wiggs, C.L., Martin, A., 1998. Properties and mechanisms of perceptual priming. Curr. Opin. Neurobiol. 8, 227–233.
Wiggs, C.L., Weisberg, J., Martin, A., 1999. Neural correlates of semantic and episodic memory retrieval. Neuropsychologia 37, 103–118.
Wilson, M.D., 1988. The MRC psycholinguistic database: machine readable dictionary, version 2. Behav. Res. Methods Instrum. Comput. 20, 6–11.
Yang, Z., Chang, C., Xu, T., Jiang, L., Handwerker, D.A., Castellanos, F.X., Milham, M.P., Bandettini, P.A., Zuo, X., 2014. Connectivity trajectory across lifespan differentiates the precuneus from the default network. Neuroimage 89, 45–56.
Yeo, B.T.T., Krienen, F.M., Sepulcre, J., Sabuncu, M.R., Lashkari, D., Hollinshead, M., Roffman, J.L., Smoller, J.W., Zollei, L., Polimeni, J.R., 2011. The organization of the human cerebral cortex estimated by intrinsic functional connectivity. J. Neurophysiol. 106, 1125–1165.